Journal of Human Evolution 65 (2013) 479–489

Contents lists available at ScienceDirect

Journal of Human Evolution

journal homepage: www.elsevier.com/locate/jhevol

A 3-D geometric morphometric study of intraspecific variation in the ontogeny of the temporal bone in modern *Homo sapiens*

Heather F. Smith [a,b,*], Terrence Ritzman [b,c], Erik Otárola-Castillo [d,e], Claire E. Terhune [f]

[a] Department of Anatomy, Arizona College of Osteopathic Medicine, Midwestern University, 19555 N. 59th Ave., Glendale, AZ 85308, USA
[b] School of Human Evolution and Social Change, Arizona State University, Tempe, AZ, USA
[c] Institute of Human Origins, Arizona State University, Tempe, AZ, USA
[d] Department of Ecology, Evolution, and Organismal Biology, Iowa State University, Ames, IA, USA
[e] Department of Human Evolutionary Biology, Harvard University, Cambridge, MA, USA
[f] Department of Community and Family Medicine, Duke University, Durham, NC, USA

ARTICLE INFO

Article history:
Received 23 May 2012
Accepted 18 January 2013
Available online 12 September 2013

Keywords:
Ontogenetic trajectory
Cranial variation
Subadult temporal bone morphology

ABSTRACT

This study addresses how the human temporal bone develops the population-specific pattern of morphology observed among adults and at what point in ontogeny those patterns arise. Three-dimensional temporal bone shape was captured using 15 landmarks on ontogenetic series of specimens from seven modern human populations. Discriminant function analysis revealed that population-specific temporal bone morphology is evident early in ontogeny, with significant shape differences among many human populations apparent prior to the eruption of the first molar. As early as five years of age, temporal bone shape reflects population history and can be used to reliably sort populations, although those in closer geographic proximity and molecular affinity are more likely to be misclassified. The deviation of cold-adapted populations from this general pattern of congruence between temporal bone morphology and genetic distances, identified in previous work, was confirmed here in adult and subadult specimens, and was revealed to occur earlier in ontogeny than previously recognized. Significant differences exist between the ontogenetic trajectories of some pairs of populations, but not among others, and the angles of these trajectories do not reflect genetic relationships or final adult temporal bone size. Significant intrapopulation differences are evident early in ontogeny, with differences becoming amplified by divergent trajectories in some groups. These findings elucidate how the congruence between adult human temporal bone morphology and population history develops, and reveal that this pattern corresponds closely to that described previously for facial ontogeny.

Introduction

Several studies investigating modern human cranial variation have revealed a now well-established relationship between cranial morphology and population history in our species, i.e., that linear dimensions of the skull largely reflect genetic distances among human populations (Relethford, 1998, 2001; Roseman, 2004). Likewise, three-dimensional (3D) shape, as captured by geometric morphometric analyses, has been shown to accurately mirror population history for both functional and developmental modules of the skull (Harvati and Weaver, 2006; von Cramon-Taubadel, 2009a, 2011), as well as individual cranial bones (Harvati and Weaver, 2006; Smith et al., 2007; Smith, 2009; von Cramon-Taubadel, 2009b). However, few studies have evaluated how the congruence between cranial morphology and genetic distances develops during ontogeny. Thus, the process by which this pattern emerges remains unclear. The purpose of the present study is to investigate the relationship between ontogenetic patterns and molecular distances for one particular cranial region in humans, the temporal bone.

Temporal bone morphology, genetic distances, and the role of ontogeny

Many studies have focused on the 3D morphology of the temporal bone in both humans (Harvati and Weaver, 2006; Smith et al., 2007; Smith, 2009; von Cramon-Taubadel, 2009b) and non human primates (Lockwood et al., 2002, 2004; von Cramon-Taubadel and Smith, 2012). Comparisons of temporal bone shape to either molecular or geographic distances have consistently revealed that

* Corresponding author.
E-mail addresses: hsmith@midwestern.edu, heather.f.smith@asu.edu (H.F. Smith).

0047-2484/$ – see front matter © 2013 Elsevier Ltd. All rights reserved.
http://dx.doi.org/10.1016/j.jhevol.2013.01.017

temporal bone morphology reliably reflects population history among humans (Harvati and Weaver, 2006; Smith et al., 2007; Smith, 2009; von Cramon-Taubadel, 2009b). Among hominoids, temporal bone morphology has been found to mirror phylogenetic relationships among taxa, even down to the level of the subspecies (Lockwood et al., 2002, 2004; von Cramon-Taubadel and Smith, 2012).

Possible explanations for the congruence between basicranial (including temporal bone) morphology and genetic relatedness have been extensively discussed (Olson, 1981; MacPhee and Cartmill, 1986; Lieberman et al., 1996, 2000a; Lieberman, 1997; Smith et al., 2007; Smith, 2009; von Cramon-Taubadel and Smith, 2012), and one reason for this congruence may be the pattern of temporal bone development. In essence, many components of the temporal bone approximate their adult form by the time an infant comes to term. Much of this ossification derives from a stable cartilaginous template, rather than an intramembranous template (found in many bones of the neurocranium and splanchnocranium), which is more prone to plasticity during development (Olson, 1981; MacPhee and Cartmill, 1986; Lieberman et al., 1996, 2000a). The basicranium (of which the temporal bone is part) also closely mirrors the shape of the developing brain, which is highly morphologically constrained (de Beer, 1937; Weidenreich, 1941; Babineau and Kronman, 1969; David et al., 1990).

The remaining ossification of the temporal bone occurs relatively early in childhood, from eight distinct ossification centers, plus those of the tympanic ring and auditory ossicles (White and Folkens, 2000). The endochondrally-ossifying petrous pyramid and middle ear bones, as well as portions of the intramembranously ossifying squama and tympanic, almost exclusively ossify prenatally (Scheuer and Black, 2000). Temporal bone development also involves several stages of pneumatization through three primary centers: the mastoid antrum, mastoid center, and petrous portion (Bast and Forester, 1939; Allam, 1969; Sherwood, 1995; Kenna, 1996). By late adolescence, the glenoid and mastoid process have reached their final adult size and proportions, and the development of the entire temporal bone ceases (Eby and Nadol, 1986; Scheuer and Black, 2000).

Relationship between the morphology of other cranial regions and genetic distances

Although the temporal bone appears to reflect genetic distances among populations and species, current evidence suggests that not all cranial regions and bones reflect population history equally reliably. Some researchers have suggested that the morphology of the entire facial skeleton accords less consistently with these relationships than regions such as the temporal bone and neurocranium (Harvati and Weaver, 2006). Smith (2009) showed that the morphology of the upper face is congruent with population history, but that the morphology of the maxilla and mandible are not. These findings coincide with those of previous researchers (Howells, 1990; Roseman, 2004; von Cramon-Taubadel, 2009b). Specifically, they reveal that while many aspects of cranial morphology reflect molecular distances in *Homo sapiens*, some aspects of facial shape are more reliable indicators of genetic relatedness than others. For example, the upper face reflects genetic distances consistently, but the alveolar bone surrounding the oral apparatus deviates from an expected pattern of congruence with molecular relationships, presumably due to the masticatory strain it experiences.

As both the temporal bone (as part of the temporomandibular joint) and facial skeleton are components of the masticatory system, they may both be expected to deviate from such patterns of congruence. The role of masticatory strain, its potential impact on phenotypic plasticity, and the degree to which that might affect its phylogenetic utility has been recently discussed (Lieberman, 1995; Lieberman et al., 1996, 2000b; Lieberman, 1997; Collard and Wood, 2001; Lycett and Collard, 2005; Collard and Wood, 2007; von Cramon-Taubadel, 2009a, 2011). Lieberman initially hypothesized that cranial regions experiencing higher strains during mastication would be less useful for reconstructing phylogeny (Lieberman, 1995; Lieberman et al., 1996; Lieberman, 1997). This 'homoiology hypothesis' was not supported, however, when the masticatory and non-masticatory regions of the skull in papionins were found to be equally congruent with the molecular phylogeny of papionins (Lycett and Collard, 2005). Subsequent studies have since reaffirmed the idea that masticatory and non-masticatory regions are equally reliable for reconstructing phylogeny among hominoid species (Collard and Wood, 2007) and human populations (von Cramon-Taubadel, 2009a, 2011). Thus, neither the morphology of the temporal bone nor facial skeleton should be inferred to be unreliable for reconstructing phylogeny.

Patterns of cranial ontogeny in humans and the great apes

Few studies have tracked developmental changes in the 3D form of specific aspects of human cranial morphology. Strand Viðarsdóttir et al. (2002) reported that patterns of variation in the facial skeleton of *H. sapiens* from diverse geographic populations are evident very early postnatally, but that differences in postnatal ontogenetic trajectories among these populations also contribute to variation in adults. In other words, although population-specific morphologies may be present in the human face at birth, these differences are magnified by differences in the timing and direction of morphological change during postnatal ontogeny, as evidenced by divergent ontogenetic trajectories. Furthermore, using geographic distribution as a proxy for population history, Strand Viðarsdóttir et al. (2002) concluded that population-specific ontogenetic trajectories do not mirror population history, in that populations from geographically distant areas do not exhibit more divergent trajectories than those in closer geographic proximity. However, given that not all components of the facial skeleton consistently reflect population history in humans (Harvati and Weaver, 2006; Smith, 2009; von Cramon-Taubadel, 2009b), it remains unclear whether these findings would also apply to separate parts of the facial skeleton or to other cranial regions.

An important consideration is that previous studies comparing temporal bone morphology and genetic distances were conducted exclusively on adult samples; thus, it is currently unknown at what stage during ontogeny the temporal bone begins to reflect genetic relatedness. Several scenarios could explain variations in adult temporal bone morphology: subadults from different populations may all exhibit similar temporal bone morphology that subsequently develops into different adult shapes via divergent ontogenetic trajectories, or temporal bone morphology may reflect genetic relatedness very early in ontogeny, with these differences maintained throughout ontogeny by developing along similar (i.e., parallel) trajectories. A third scenario is that neither of these explanations can fully describe temporal bone ontogeny and that both processes are acting in concert. Thus, for instance, Terhune and colleagues (Terhune et al., 2013) recently concluded that temporal bone morphology in African apes and humans is distinct early in development, and departs further via divergent ontogenetic trajectories.

These data therefore set the stage for the questions: how does the morphology of the human temporal bone come to reflect adult intraspecific population history, and does human temporal bone growth and development follow the same pattern described for the African apes? This also raises the question of scale: specifically, whether interspecific and intraspecific patterns of temporal bone

ontogeny are similar. Since evolutionary processes may affect phenomena above and below the species level in different ways, it is possible that the ontogenetic patterns observed at these scales may differ – a hypothesis that requires testing.

Hypotheses

In light of the previous work, the present study seeks to determine when during ontogeny population-specific temporal bone morphologies emerge, and to compare temporal bone ontogeny among human populations. We test the following hypotheses:

H1a. Human populations differ significantly in the shape of the temporal bone irrespective of maturation. As a corollary to H1a, the following hypothesis was also tested: **H1b**. Differences in temporal bone shape among sub-adult populations reflect their molecular differences.

H2a. Human populations differ significantly in the orientation and/or length of their ontogenetic trajectories in morphospace.

H2b. These ontogenetic trajectory differences reflect the molecular distances among populations.

Materials and methods

Data collection

Three-dimensional landmarks describing temporal bone morphology were collected from ontogenetic series from seven modern human populations (Table 1). These populations represent a geographically diverse sample and were chosen based on two criteria: (1) having a close molecular representative that is well-typed for neutral molecular loci, and (2) having sufficient ontogenetic series available in museum collections (American Museum of Natural History and National Museum of Natural History). Published molecular data on microsatellites, or short tandem repeats (STRs), on closely-related molecular representative populations were obtained from Rosenberg et al. (2005). The practice of utilizing the best representative molecular data for each skeletal population has been employed by several previous studies (Roseman, 2004; Harvati and Weaver, 2006; Smith et al., 2007; Smith, 2009; von Cramon-Taubadel, 2009a, b), and it has been argued that any mismatch therein should lead to a minimum estimate of the concordance between molecular and morphological data (Roseman, 2004).

Each subadult specimen was assigned a developmental age estimate to the nearest year based on established dental eruption standards (Ubelaker, 1989). Adult status was based on eruption of the third molars and/or fusion of the spheno-occipital synchondrosis. Following Strand Viðarsdóttir et al. (2002), all adult specimens were assigned the age of 21 years. The adult samples consist of roughly equal numbers of male and female individuals for each population. Only specimens with no apparent pathology or antemortem tooth loss were included in the study. To ensure that the subadult samples for each population had roughly similar age distributions, subadults were assigned an ontogenetic category as follows: 1 = M1s not yet erupted, 2 = M1s erupted but not M2s, 3 = M2s erupted but not M3s, 4 = adult, M3s erupted and/or spheno-occipital synchondrosis fused.

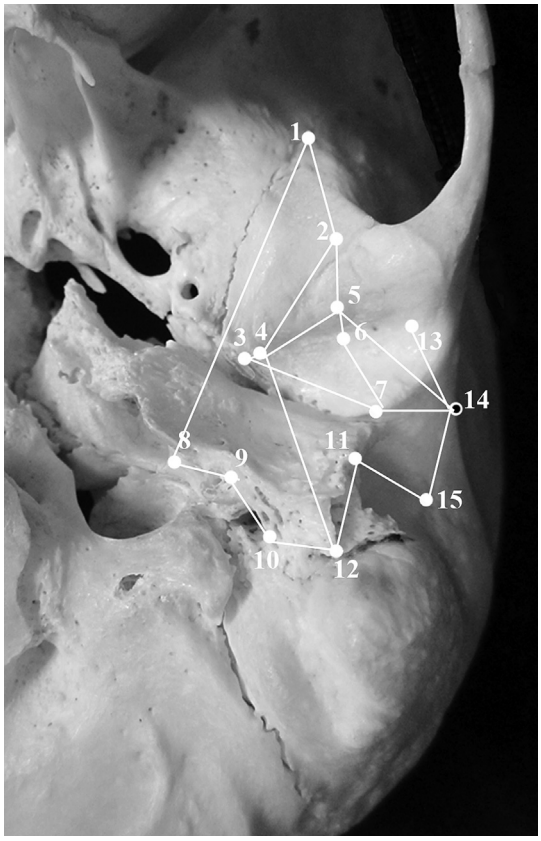

Figure 1. Fifteen temporal bone landmarks digitized in the present study, following Lockwood et al. (2004). Please see Table 2 for landmark definitions. The open circle for landmark #14 indicates its approximate position, as it is not directly visible from this perspective.

Fifteen landmarks capturing the 3D shape of the ectocranial surface of the temporal bone (Fig. 1; Table 2) were digitized using a Microscribe G2 digitizer (Immersion Corp., San Jose) by HFS. These landmarks derive initially from Lockwood et al. (2002), and subsets thereof have been used subsequently to quantify temporal bone morphology in previous studies of temporal bone shape in adult humans (Smith et al., 2007; Smith, 2009). While these landmarks

Table 1
Human population samples included in the present study, their adult and subadult sample sizes, and molecular representative populations.

	Category 1 subadults	Category 2 subadults	Category 3 subadults	Total subadults	Adults[a]	Total	Molecular representative
Alaska	5	8	4	17	10	27	Siberians
Austria	4	20	14	38	11	49	French
Egypt	11	10	9	30	11	41	Mozabite
Mexico	11	14	3	28	10	38	Maya
Peru	6	6	9	21	11	32	Colombians
Polynesia	6	6	4	16	10	26	Solomon Islanders
Utah	6	4	3	13	10	23	Pima

All population samples were derived from the American Museum of Natural History (New York, NY) or the National Museum of Natural History (Washington, DC).
[a] Adult samples of 10 specimens consisted of five males and five females. Adult samples of 11 specimens contained one more specimen of one sex. Subadult specimens could not be sexed.

Table 2
Definitions of temporal bone landmarks digitized. From Lockwood et al. (2004).

No.	Definition
1	Intersection of the infratemporal crest and sphenosquamosal suture
2	Most anterior point on the articular surface of the articular eminence
3	Most inferior point on entoglenoid process
4	Most inferior point on the medial margin of the articular surface of the articular eminence
5	Center of the articular eminence
6	Deepest point within the mandibular fossa
7	Most inferior point on the postglenoid process
8	Most posterolateral point on the margin of the carotid canal entrance
9	Most lateral point on the vagina of the styloid process (whether process is present or absent)
10	Most lateral point on the margin of the stylomastoid foramen
11	Most inferior point on the external acoustic porus
12	Most inferolateral point on the tympanic element of the temporal bone
13	Point of inflection where the braincase curves laterally into the supraglenoid gutter, in coronal plane of the mandibular fossa
14	Point on lateral margin of the zygomatic process of the temporal bone at the position of the postglenoid process
15	Porion

have not been employed previously in studies of subadult specimens, it should be noted that they were found here to be readily identifiable even at the early stages of ontogeny. An intraobserver error analysis indicated no significant error for these landmarks in adults, with error rates ranging from less than 1.00 mm–2.50 mm (average: 1.75 mm).

Analytical methods

Differentiation and classification among populations Raw coordinate data were first subjected to generalized Procrustes analysis (GPA) and principal components analysis (PCA) using MorphoJ (Klingenberg, 2011) both for the entire sample and for each age subset of cranial data. Shape variation in the sample was visualized using wireframe diagrams (as shown in Fig. 1), and by warping the mean shape configuration along each of the major PC axes. We determined which PCs were significantly correlated with developmental age and size by regressing the PC scores against our developmental age estimate and against the natural log of centroid size. We use centroid size (defined as the sum of the squared distances from each landmark to the centroid of the shape configuration) here as a rough measure of overall cranial size. By regressing the PC scores against developmental age we examine growth of the temporal bone, and by regressing the PC scores against centroid size we assess ontogenetic allometry.

To assess whether populations differed significantly in morphospace, we used the Procrustes rotated coordinates (i.e., Procrustes residuals) to calculate a matrix of Procrustes distances among populations for several subsets of the entire sample: separately for each age category, subadults only (categories 1, 2, and 3 combined), and a combined age sample (all age categories together). The significance of the pairwise distances between populations was assessed using a permutation test with 10,000 replicates; *p*-values were calculated as the number of times the original Procrustes distance between populations was exceeded, divided by the total number of iterations. We assessed whether subadult and adult patterns of morphological differentiation were consistent with one another by performing a Mantel test (Mantel, 1967) to examine the correlation between the matrix of adult Procrustes distances and the matrices describing subadult differences (e.g., the matrices for each age category and the matrix for the combined subadult sample). Procrustes distances among populations based on adult morphology were then compared with those based on each of the subadult categories (age categories 1, 2, 3, and the combined subadult sample) using a Mantel test (Mantel, 1967) to determine whether subadult temporal bone shape patterns reflected adult patterns. Some authors have used Mahalanobis D^2 distances as measures of intergroup differences for cranial landmark-based data in humans (Strand Viðarsdóttir et al., 2002; Harvati and Weaver, 2006; Smith et al., 2009; von Cramon-Taubadel, 2009a, b; von Cramon-Taubadel and Smith, 2012); however, the relatively small sizes of the current age categories render Procrustes distances more robust in the present study since they do not assume similarities in covariance structures among groups, whereas Mahalanobis does (Klingenberg and Montiero, 2005).

Discriminant function analyses (DFA) with cross-validation were performed to examine the degree to which temporal bone morphology can be utilized to classify individuals of various ages into the correct population, and to shed light on when population-specific differences appear during ontogeny. Discriminant function analyses were conducted using PASW 18 (IBM Corp., Somers, NY) and the higher-order PCs that explain 95% of the variance (PCs 1-24 for adults, PCs 1-26 for subadults, and PCs 1-27 for the entire sample). Separate analyses were performed for the adults (category 4) only, subadults (categories 1–3 combined), and the combined adult and subadult sample. Sample sizes were not sufficient for this analysis to be conducted for each subadult age category separately.

Molecular relationships versus temporal bone shape To assess whether temporal bone shape mirrors molecular relationships among modern human populations of various ages, the molecular distances between population samples were compared to morphological (Procrustes) distances. Using Arlequin 3.11 (Excoffier et al., 2005), molecular fixation index (F_{ST}) distances among groups were calculated using data on 783 microsatellites for the molecular representative populations (as made available by Rosenberg et al. (2005)). The F_{ST} is a statistic that compares the degree of genetic variation of two or more groups compared with that of the entire sample (Wright, 1965). It is calculated as: $F_{ST} = (H_T - H_S)/H_T$, in which H_T is the average expected amount of heterozygosity in the entire sample, and H_S is the expected amount of heterozygosity within a population (Wright, 1965). A matrix of molecular distances among populations was subsequently compared to the matrices of Procrustes distances for each subadult age category, the combined subadult sample, and adult-only subsets of the sample using Mantel tests (Mantel, 1967). Since there has been extensive debate in the literature about the use of Procrustes versus Mahalanobis distances in analyses such as these (Ackermann, 2002, 2005; Klingenberg and Montiero, 2005), the analysis was run a second time using Mahalanobis distances to assess whether the choice of distance measure would impact the results.

Some researchers suggest that human populations living in extremely cold climates may have undergone both adaptive and plastic responses to feeding and/or paramasticatory behaviors that have caused their basicrania to differ substantially from those of non-cold-adapted populations (Hylander, 1977; Harvati and Weaver, 2006). Specifically, Hylander (1977) found that the tympanic plate of Alaskan Eskimos is thickened, likely as an adaptation to the long-term functional pressures of a diet of tough and partially frozen items. The unique paramasticatory behaviors documented ethnographically in these populations likely also result in plastic responses to the morphology of the temporomandibular joint during the individual's lifetime (such as remodeling of the mandibular fossa and other aspects of the TMJ), similar to other plastic changes of the masticatory apparatus that have been described, such as the development of

mandibular and palatal tori (Hylander, 1977). Because of the potential for such populations to confound our analysis, we followed Harvati and Weaver (2006) and conducted the Mantel tests a second time without the Alaskan population. In doing so, we determined whether the inclusion of a cold-adapted sample affected the correlation between temporal bone morphology and molecular distances in subadults, as has been previously shown for adults (Harvati and Weaver, 2006; Smith et al., 2007; Smith, 2009).

Ontogenetic trajectories in morphospace Multiple analyses were conducted to compare the trajectories of shape change in morphospace among the populations in the sample. First, we quantified the trajectory of shape change relative to size (i.e., ontogenetic allometry) in morphospace for each population using multivariate regression analysis. For this analysis, we first superimposed all specimens in the dataset so that all populations were in the same morphospace. We then regressed shape (i.e., all Procrustes residuals) on the natural log of centroid size. This regression was performed separately for each population in the dataset. The regression coefficients for the dependent variables (x1, y1, z1, x2, y2, z2, … x15, y15, z15) then describe a population-specific vector of shape change relative to size (Anderson and Ter Braak, 2003; Collyer and Adams, 2007; Adams and Collyer, 2009; Piras et al., 2010). Angles between these vectors (which in an ontogenetic sample represent ontogenetic allometric trajectories) for each pair of populations (e.g., Alaskans versus Polynesians) were calculated as the arccosine of the dot product of the vectors, and a matrix of these angles was compiled. The significance of each angle was evaluated using a permutation test (with 9,999 iterations), in which group membership was randomly shuffled but the sample sizes for each age category were held constant (McNulty et al., 2006). *P*-values were calculated as the number of times the original regression residual was exceeded, divided by the total number of iterations. These analyses were conducted using code modified by EO-C from the R package 'geomorph' (Adams and Otárola-Castillo, 2012, 2013).

To visualize the differences in these angles among pairs of taxa, we performed a multidimensional scaling analysis using PASW Statistics 18 (IBM Corp., Somers, NY). A multidimensional scaling analysis plots a given matrix of distances in *n*-dimensional space (here, $n = 3$), in order to facilitate a visualization of intergroup distances. Following Strand Viðarsdóttir et al. (2002), a Student's *t*-test of centroid sizes was conducted between each pair of populations to determine whether significant differences existed in size among adults. Examining differences in adult size may suggest the existence of differences among populations in the timing and/or rate of temporal bone growth. Finally, we used a Mantel test to compare the matrix of angles between the ontogenetic trajectories to the molecular distance matrix and to a matrix of absolute differences in adult centroid size. This analysis allowed us to determine whether patterns of ontogenetic trajectory divergence reflected molecular distances and/or final adult size among populations.

Because of the high number of statistical tests employed in this study, we guard against Type-I error by performing a sequential Bonferroni adjustment of the *p*-values (Rice, 1989) for each separate analysis. A sequential Bonferroni is conducted by ranking the significance values from a set of multiple comparisons from smallest to largest. The alpha value, in this case $\alpha = 0.05$, is divided by the inverse of the rank of each significance value to determine the corrected *p*-value. The current study contained 20 pairs of populations, and thus, 20 *p*-values were calculated for each matrix of distances. Thus, for example, for the fifth largest *p*-value in a given matrix, the critical alpha would be $0.05/16 = 0.003125$. The details of the resulting significance values will be discussed below with the relevant results.

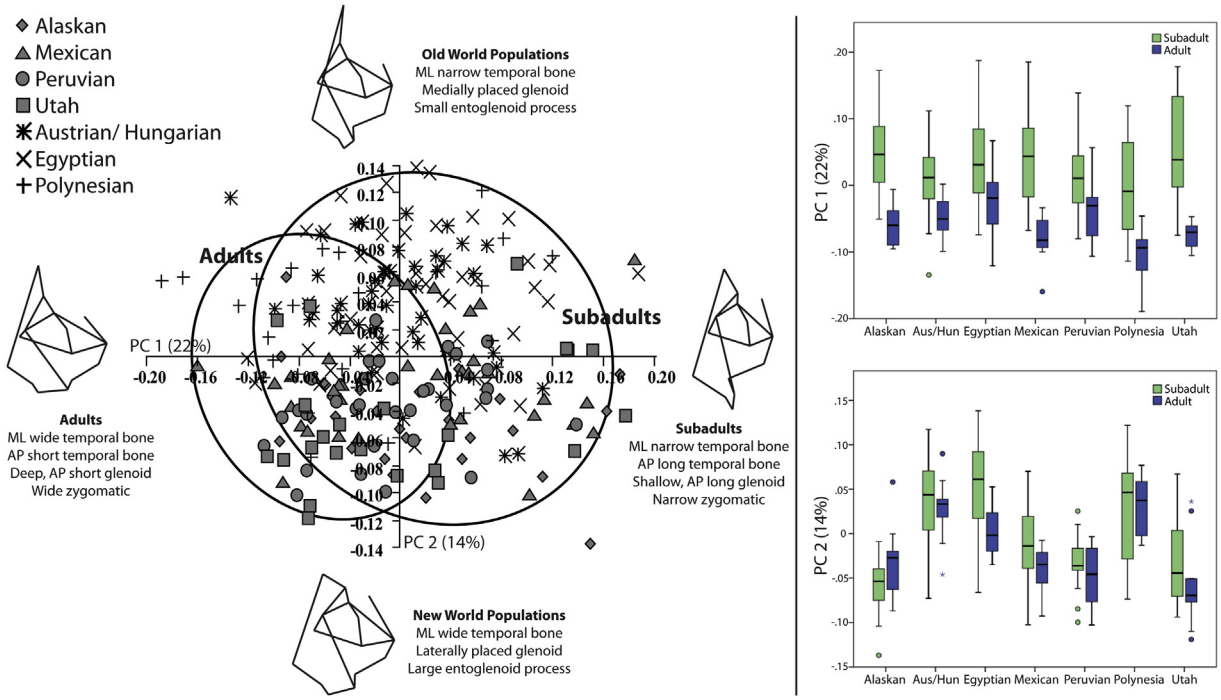

Figure 2. Bivariate plot of PC axes one (*x*-axis) and two (*y*-axis) showing population and age variation in the sample. Confidences ellipses encompass 90% of the shape variation for the subadult and adult samples. Box plots on the right hand side of the figure show the distribution of PC scores for PC axes 1 (top) and 2 (bottom) by population and for the subadult and adult samples separately. Darkened bars represent the median for each group, the boxes indicate the interquartile range (25th–75th percentiles), and the whiskers extend to 1.5 times the interquartile range. Outliers are indicated by circles and extremes are indicated by asterisks.

Results

Differentiation and classification among populations

Visualization of variation in shape space using PCA reveals what one might expect for an intraspecific analysis such as this: there are few discrete groupings of populations or age categories along the top PC axes (Figs. 2 and 3; Table 3). However, examination of the placement of age categories and populations does reveal several interesting patterns in the shape variation. Axis 1 (which explains 22% of the sample variance and is significantly correlated with both biological age and natural log centroid size) primarily represents shape variation related to ontogeny; subadults tend to load positively on this axis whereas adults tend to load negatively, although there is still considerable overlap in these two groups along this axis (Figs. 2 and 3). Warping the mean shape configuration along this axis revealed that shape variation on PC 1 represents changes in the mediolateral width and anteroposterior length of the temporal bone, as well as changes in the glenoid and zygomatic portions of the temporal bone.

Interestingly, PC 2 appears to be related to differences in temporal bone shape among New and Old World populations (Fig. 2), and is not correlated with age or size. Examination of the warped wireframe diagrams along PC2 indicated that the New World populations (Alaskans, Mexicans, Peruvians, and Utah Native Americans), which load more negatively on this axis, have a relatively mediolaterally wide temporal bone with a laterally placed glenoid and large entoglenoid process. In contrast, the warped wireframe diagrams indicate that the Old World populations (Austrian/Hungarians, Egyptians, and Polynesians), which load more positively on PC2, have relatively mediolaterally narrower temporal bones with more medially placed glenoids and small entoglenoid processes. There may also be a component of ontogenetic shape variation along this axis, as more adults tend to load negatively than subadults along PC 2 in all populations except the Alaskans.

Although populations do not appear distinct in the PC plot shown (Fig. 2), Procrustes distances between the population means were found to be significantly different in almost all cases (Table 4). This was true for both the combined subadult sample and the adult sample, even when a sequential Bonferroni adjustment had been applied (Table 4). Procrustes distances were also significantly different when each age category (age categories 1–3) was examined separately suggesting morphological separation from an early age. In particular, in age category 1 all populations were significantly different, except for the following pairs: Alaska/Mexico, Alaska/Utah, Mexico/Peru, Mexico/Utah, Peru/Utah (i.e., 23.8% of pairwise comparisons were not significant). For age category 2, all populations were significantly different except Alaska/Utah and Mexico/Peru (9.5% of comparisons). The only non-significant pairs in age category 3 were Alaska/Mexico, Alaska/Peru, Alaska/Utah, Mexico/Utah, Polynesia/Egypt, and Polynesia/Utah (28.6% of comparisons). This result represents partial support for H1a, that human populations are significantly different in temporal bone morphology irrespective of maturity, and further suggests that population differences in temporal bone morphology are present very early in ontogeny.

When Mantel tests were used to assess whether the pattern of Procrustes distances among the adult and subadult matrices were consistent, the majority of the matrices were significantly correlated: adults versus age category 1: $r = 0.876$, $p < 0.001$; adults versus age category 2: $r = 0.379$, $p = 0.075$; adults versus age category 3: $r = 0.559$, $p = 0.011$; adults versus combined subadult sample: $r = 0.770$, $p = 0.001$. After the sequential Bonferroni correction, all comparisons were significant except adults versus age category 2. This result further suggests that the pattern of adult shape differences is established early in ontogeny.

Table 3
Loadings of principal components (PCs) from the combined age sample, and their correlations with natural log centroid size and biological age (in years).

PC	% variance	Cumulative	Correlation with ln centroid size	Correlation with age
PC1	22.197	22.197	***r* = −0.746**	***r* = −0.740**
PC2	13.818	36.015	$r = 0.039$	$r = 0.114$
PC3	7.673	43.688	***r* = 0.210**	$r = -0.047$
PC4	5.704	49.392	***r* = 0.134**	***r* = 0.336**
PC5	5.452	54.844	$r = 0.009$	$r = -0.106$
PC6	4.484	59.328	$r = -0.051$	$r = -0.030$
PC7	3.899	63.227	$r = -0.055$	$r = -0.083$
PC8	3.528	66.756	$r = -0.085$	$r = -0.033$
PC9	2.991	69.747	$r = -0.006$	$r = -0.015$
PC10	2.658	72.404	$r = 0.012$	$r = -0.083$
PC11	2.352	74.756	$r = 0.121$	***r* = 0.137**
PC12	2.227	76.984	$r = -0.007$	$r = 0.091$
PC13	2.097	79.081	$r = 0.079$	$r = -0.017$
PC14	1.846	80.927	$r = 0.067$	$r = 0.009$
PC15	1.795	82.722	$r = 0.066$	$r = 0.001$

Significant correlations are indicated in bold.

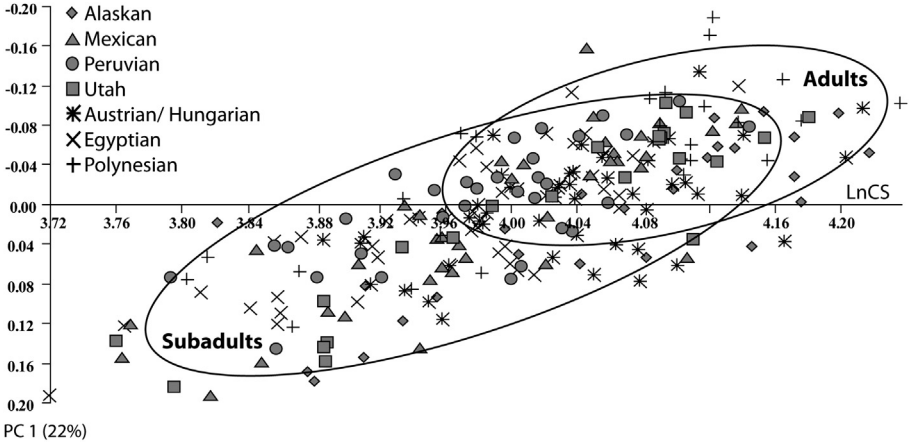

Figure 3. Bivariate plot showing the natural log of centroid size (LnCS, *x*-axis) and the first PC axis (*y*-axis) ($r = 0.754$, $p < 0.001$). Confidence ellipses encompass 90% of the shape variation for the subadult and adult samples.

Table 4
Morphological (Procrustes) distance matrix among populations based on temporal bone morphology of adults (top triangle) and subadults (bottom triangle).

	Alaska	Austria	Egypt	Mexico	Peru	Polynesia	Utah
Alaska	–	**0.1137***	**0.1293***	**0.0855***	**0.1074***	**0.1194***	**0.0942***
Austria	**0.1163***	–	**0.0827***	**0.0939***	**0.1035***	**0.1032***	**0.1073***
Egypt	**0.1320***	**0.0687***	–	**0.1144***	**0.0871***	**0.1105***	**0.1012***
Mexico	**0.0706***	**0.0734***	**0.0946***	–	**0.0765***	**0.1017***	0.0621
Peru	**0.0794***	**0.0872***	**0.1042***	**0.0539**	–	**0.1204***	**0.0664***
Polynesia	**0.1162***	**0.0772***	**0.0771***	**0.0951***	**0.0951***	–	0.1128
Utah	0.0657	**0.1093***	**0.1131***	0.0529	0.0671	**0.1208***	–

Lower triangle matrix depicts distances based on subadult morphology (categories 1–3 combined), and upper matrix depicts distances based on adult morphology. Significant differences are indicated in bold, and asterisks indicate differences that were also significant after the sequential Bonferroni correction.

The DFA for the adult sample resulted in cross-validated classification rates ranging from 30% to 80% (Table 5). The highest rates of misclassification occurred between the New World populations. The DFA for the subadult sample indicated a wide range of correct classification, with between 7.7 and 65.8% of the individuals correlated classified to population (Table 6). The populations with the lowest correct classification rates, Utah (7.7%) and Mexico (28.6%), were both more likely to be misclassified as another New World population than a group derived from a different geographic region (Table 6). The combined age sample resulted in 21.7–63.0% correct classification to population (Table 7).

Correspondence between molecular relationships and temporal bone shape

The molecular F_{ST} distances based on microsatellite data are consistent with those found in previous studies (Roseman, 2004; Rosenberg et al., 2005). Results of the Mantel tests between F_{ST} distances and the Procrustes distances are presented in Table 8. In sum, there was a significant correlation between molecular and morphological distances for the 'all ages' category, but only when the cold-adapted population was removed (Table 8). Inclusion of the cold-adapted population resulted in significant correlations for age categories 2 and 3, and a marginally significant correlation for the combined subadult sample (Table 8). This result provides support for H1b, that the differences in temporal bone shape among populations reflect their molecular distances; however, this is only true when the cold-adapted populations are excluded. Using Mahalanobis distances instead of Procrustes distances resulted in similar results ($r = 0.415$, $p = 0.035$ for the entire combined subadult sample; $r = 0.163$, $p = 0.287$ for the adult sample).

Ontogenetic trajectory comparison

Pairwise differences in the angles between ontogenetic allometric trajectories are reported in Table 9. The largest number of angular differences are between the Austrian population and several of the other populations (bottom half of Table 9): Peru (66.444°), Utah (59.021°), Polynesia (54.304°), and Egypt (54.303°) (Table 9). There were also dramatic differences between the Polynesian sample and several others: Austria (54.304°), Peru (47.947°), Utah (46.127°), and Egypt (44.012°) (Table 9). Several populations were found to differ significantly in the angles of their trajectories at $p < 0.05$, although only two angles remained significant after the sequential Bonferroni correction (Austria versus Peru and Polynesia versus Utah).

This result provides partial support for the hypothesis (H2a), that differences in adult temporal bone morphology are achieved, at least in part, by divergent postnatal ontogenetic trajectories. In particular, trajectories for the Polynesians differed from all other populations except the Alaskan and Mexican samples, although only the difference with the Utah sample remained significant after the more conservative sequential Bonferroni correction (Table 9). The Austrians also differed from the Egyptians, Peruvians, and Utah Native Americans, although only the comparison with the Peruvians remained significant after the sequential Bonferroni correction (Table 9). The Peruvians also differed from the Alaskans, although again this comparison was not significant after sequential Bonferroni correction (Table 9). Thus, the most divergent ontogenetic trajectories appear to be for the Austrians and Polynesians, since their angles differ from the largest number of populations, although few of these differences remain significant after the Bonferroni correction. The multidimensional scaling analysis further revealed the divergence of the Polynesian and Austrian populations (Fig. 4).

In contrast, considerably more pairs of taxa differed significantly in adult centroid size (top triangle in Table 9). Thirteen of the 21 population pairs were significantly different in size at $p < 0.05$, with seven of these values remaining significant after sequential Bonferroni correction. Of these corrected values, three differences involved the Alaskan sample, which was significantly larger than the Egyptian, Mexican, and Peruvian samples. The Egyptian sample was also significantly smaller than the Polynesians and Utah Native Americans, as were the Peruvians (Table 9).

There was no significant correlation between the matrix of ontogenetic trajectories and the molecular distance matrix ($r = 0.101$, $p = 0.373$), suggesting that these trajectories do not reflect inter-population molecular relationships. This finding indicates a lack of support for H2b, that the angles of human ontogenetic trajectories will reflect the genetic relatedness among populations. The patterns of ontogenetic trajectories were also uncorrelated with both subadult ($r = 0.109$, $p = 0.366$) and adult Procrustes distances ($r = 0.350$ $p = 0.116$), and adult centroid size ($r = 0.250$, $p = 0.206$).

Discussion

Multiple previous studies have revealed a correlation between temporal bone shape and genetic distances in humans

Table 5
Classification results from discriminant function analysis with cross-validation for adult samples. Values indicate the number of specimens attributed to each population in the DFA results.

	% correct	Prior probability (%)[a]	Alaska	Austria	Egypt	Mexico	Peru	Polynesia	Utah	Total
Alaska	80.0	12.7	8	0	0	1	0	0	1	10
Austria	45.5	15.5	0	5	4	0	1	0	1	11
Egypt	36.4	14.1	0	2	4	1	2	1	1	11
Mexico	50.0	14.1	0	1	0	5	0	1	3	10
Peru	54.5	15.5	0	0	1	2	6	0	2	11
Polynesia	40.0	14.1	2	1	2	0	0	4	1	10
Utah	30.0	14.1	1	0	0	2	3	1	3	10

[a] Prior probabilities were set equal to group size.

Table 6
Classification results from discriminant function analysis with cross-validation for subadult samples. Values indicate the number of specimens attributed to each population in the DFA results.

	% correct	Prior probability (%)[a]	Alaska	Austria	Egypt	Mexico	Peru	Polynesia	Utah	Total
Alaska	52.9	10.5	9	1	0	1	1	1	4	17
Austria	65.8	23.5	1	25	4	3	4	1	0	38
Egypt	56.7	18.5	1	6	17	1	1	2	2	30
Mexico	28.6	17.3	3	4	3	8	6	0	4	28
Peru	42.9	13.0	1	1	2	7	9	0	1	21
Polynesia	53.3	9.3	0	0	4	1	2	8	0	15
Utah	7.7	8.0	2	0	1	7	2	0	1	13

[a] Prior probabilities were set equal to group size.

(Harvati and Weaver, 2006; Smith et al., 2007; Smith, 2009; von Cramon-Taubadel, 2009b) and phylogenetic relationships among hominoid taxa (Lockwood et al., 2002, 2004). However, the processes by which these relationships develop throughout ontogeny were not previously described for the temporal bone. Based on similar ontogenetic analyses of other cranial regions, three scenarios seem plausible under which adult human temporal bone morphology may come to reflect molecular relationships. Human populations could have achieved their adult patterns either by starting from a similar postnatal (or even prenatal) form and subsequently experiencing divergent population-specific ontogenetic trajectories, populations may reach their adult patterns early in ontogeny and develop along similar (i.e., parallel) trajectories, or the adult pattern of temporal bone morphology may be a combination of divergent ontogenetic trajectories and the establishment of prenatal differences in temporal bone form.

Temporal bone morphology and genetic relatedness throughout ontogeny

The results of this study reveal that human populations are largely characterized by significantly different temporal bone morphologies by age category 1 (i.e., prior to eruption of the M1s), as indicated by significant Procrustes distances among most pairs of populations. This suggests that substantial differences in 3D shape exist among populations at an early ontogenetic stage (Table 4). While the population sample sizes in this earliest ontogenetic category are admittedly small, we still feel that these results reveal a real biological phenomenon. Differences among populations in age category 1 also reflect the degree of difference among these populations as adults, with the exception of the Alaskan group. This finding indicates that the patterns of inter-population temporal bone morphology observed among adults originate early in ontogeny (Table 8). Importantly, strong correlations between subadult morphology and the molecular distance matrix (although only after the removal of the Alaskan sample) indicate that subadult temporal bone form reflects genetic relatedness, as it does in adults.

On the other hand, the DFA demonstrates that human subadults can be sorted into populations by temporal bone shape only somewhat reliably (Table 6). Similarly, the permutation tests of the Procrustes distances among some of the included populations (especially those from the Americas) were not statistically significant. Both of these results are suggestive that groups in closer geographic proximity have a higher likelihood of being misclassified than do more geographically distant populations. In particular, New World groups tended to have the lowest correct classification rates and were more frequently misclassified as belonging to other New World populations (Table 6). This finding implies that temporal bone morphology can be used as an indicator of genetic relatedness among subadult specimens, as it can in adults, but that overlap still exists among the morphology of some of the populations analyzed here, especially those that are in close geographic, and hence genetic, proximity. The combination of these morphological differences among populations at early ages, and similarities among populations that are closer geographically suggests that differences in ontogenetic trajectories may also play a role in the development of adult morphology.

Ontogenetic allometric trajectories

The statistical comparison of the angles between the ontogenetic allometric trajectories for each population (Table 9), as well as the multidimensional scaling visualization of the trajectories (Fig. 4) both reveal that two of the seven populations (Austrians and Polynesians) differ substantially from many of the others. The Alaskan, Mexican, Peruvian, Utah Native American, and Egyptian samples cluster together and have relatively similar trajectories. One complicating caveat of this finding, however, is that four of these five populations are from the New World, and are therefore geographically close and possibly genetically-related. While this bias cannot be avoided based on the availability of subadult specimens in museum collections, it is unclear whether the inclusion of additional populations from Europe, Asia, and Africa would reveal other shared regional trajectory patterns.

Furthermore, as indicated by the non-significant Mantel test between the matrix of angles between the ontogenetic trajectories

Table 7
Classification results from discriminant function analysis with cross-validation for combined age sample. Values indicate the number of specimens attributed to each population in the DFA results.

	% correct	Prior probability (%)[a]	Alaska	Austria	Egypt	Mexico	Peru	Polynesia	Utah	Total
Alaska	63.0	11.5	17	0	0	5	1	1	3	27
Austria	61.2	20.9	0	30	10	5	2	1	1	49
Egypt	51.2	17.4	1	10	21	1	2	4	2	41
Mexico	42.1	16.2	4	3	2	16	6	2	5	38
Peru	53.1	13.6	3	0	2	8	17	0	2	32
Polynesia	40.0	10.6	1	3	8	0	1	10	2	25
Utah	21.7	9.8	3	0	1	10	3	1	5	23

[a] Prior probabilities were set equal to group size.

Table 8
Results from the Mantel tests between morphological (Procrustes) and molecular (F_{ST}) distance matrices for all subsamples.

Group	All populations	Alaskans removed
All ages	$r = 0.364$	$\mathbf{r = 0.736}$
	$p = 0.074$	$\mathbf{p = 0.007}$
All subadults	$r = 0.354$	$\mathbf{r = 0.781}$
	$p = 0.077$	$\mathbf{p = 0.006}$
Age category 1	$r = 0.308$	$\mathbf{r = 0.628}$
	$p = 0.122$	$\mathbf{p = 0.007}$
Age category 2	$\mathbf{r = 0.383}$	$\mathbf{r = 0.671}$
	$\mathbf{p = 0.007}$	$\mathbf{p = 0.007}$
Age category 3	$\mathbf{r = 0.587}$	$\mathbf{r = 0.778}$
	$\mathbf{p = 0.007}$	$\mathbf{p = 0.001}$
Adults	$r = 0.163$	$\mathbf{r = 0.539}$
	$p = 0.287$	$\mathbf{p = 0.032}$

Significant correlations (after sequential Bonferroni adjustment) are indicated in bold.

and the molecular distance matrix, the pattern of differences/similarities in ontogenetic trajectories between populations does not strictly reflect genetic relatedness. Also, while several of the populations differ in adult centroid size, the pattern of differences in ontogenetic trajectories is not correlated directly with final adult temporal bone size. While it is conceivable that populations of larger body size might have developed along a different, possibly steeper, trajectory angle, that does not appear to be the case.

Together with the correlations between the Procrustes distance and molecular distance matrices, these results indicate that temporal bone shape reflects genetic distances before age category 1 (Table 6), but the process by which it reaches its adult form does not directly mirror genetic relationships. Temporal bone morphology is also not simply the result of allometric effects in adult temporal bones, as evidenced by the lack of correlation between centroid size and shape among populations. The likely explanation for this pattern is that the populations sampled here have different histories, and as such, are likely to have been affected by different selection pressures, may have experienced different levels of genetic drift, and/or generally may have undergone (and still be undergoing) unique evolutionary histories that shape population-specific aspects of temporal bone ontogeny.

Cold-adaptation and the Alaskan phenomenon

The inclusion of the cold-adapted Alaskan sample in the present study provides intriguing insight into the possible effects of natural selection and remodeling on temporal bone morphology. Although the Alaskans were not significantly different in temporal bone morphology from many other populations in age categories 1–3, they became significantly different from all other populations by age category 4. Thus, in the adult sample the Alaskans were

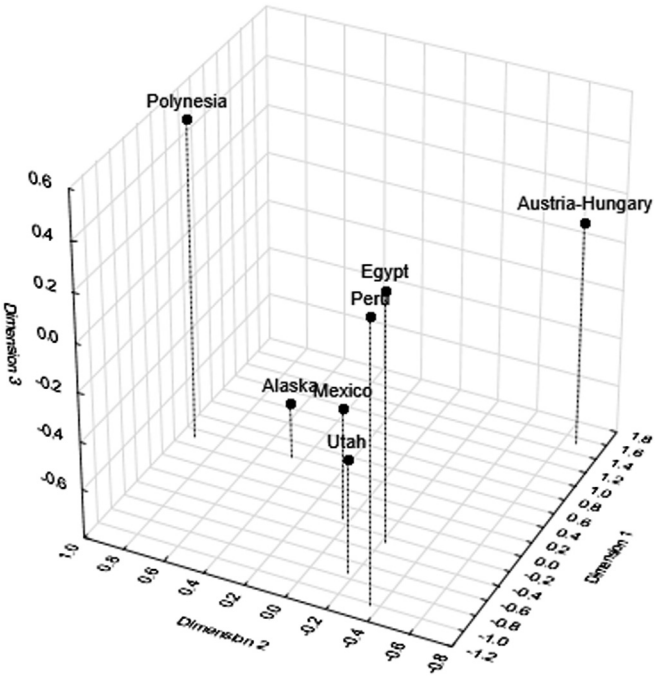

Figure 4. Three-dimensional multidimensional scaling plot summarizing dissimilarities in ontogenetic trajectory angles among populations. Stress < 0.0001. Note the divergent Polynesian and Austrian populations.

the primary deviating sample, suggesting that their divergent morphological pattern develops later in ontogeny, possibly toward the end of age category 3.

The differences between the Alaskan sample and all other groups may be at least partly explained by plastic/remodeling differences resulting from consumption of a tough, frozen diet and/or paramasticatory behaviors. Hylander (1977) described tympanic plate thickening in Alaskan Eskimos, which he argued was the result of a combination of both adaptive (selection in response to long-term functional pressures) and plastic responses (during an individual's lifetime) to dietary variables and the extraoral tooth use that typifies cold-adapted humans. The Alaskans also demonstrate the classic Bergman's Rule pattern of displaying larger average cranial (and in this case, temporal bone) sizes than the non-cold adapted populations. In fact, in the adult samples, the Alaskans were significantly larger than three of the other six populations after the Bonferroni correction. Thus, it is conceivable that the enlarged temporal bones of this population may drive the lack of correlation between temporal bone shape and genetic distances in this group.

Another interesting aspect of the Alaskan sample is that there is still a significant correlation between temporal bone shape and molecular distances when the Alaskan group is included in the age

Table 9
Ontogenetic trajectory comparisons.

	Alaska	Austria/Hungary	Egypt	Mexico	Peru	Polynesia	Utah
Alaska	–	2.223 $\mathbf{p = 0.04}$	6.525 $\mathbf{p < 0.001}^*$	4.281 $\mathbf{p = 0.001}^*$	6.202 $\mathbf{p < 0.001}^*$	1.02 $p = 0.322$	3.099 $\mathbf{p = 0.007}$
Austria/Hungary	45.498° $p = 0.082$	–	3.16 $\mathbf{p = 0.005}$	1.285 $p = 0.216$	3.068 $\mathbf{p = 0.006}$	−1.405 $p = 0.177$	0.015 $p = 0.989$
Egypt	38.529° $p = 0.192$	54.303° $\mathbf{p = 0.014}$	–	−2.187 $\mathbf{p = 0.042}$	−0.100 $p = 0.921$	−5.408 $\mathbf{p < 0.001}^*$	−4.028 $\mathbf{p < 0.001}^*$
Mexico	29.813° $p = 0.614$	48.279° $p = 0.052$	28.122° $p = 0.547$	–	2.049 $p = 0.055$	−3.199 $\mathbf{p = 0.005}$	−1.641 $p = 0.118$
Peru	51.231° $\mathbf{p = 0.018}$	66.444° $\mathbf{p = 0.002}^*$	34.158° $p = 0.552$	36.500° $p = 0.441$	–	−5.187 $\mathbf{p < 0.001}^*$	−3.794 $\mathbf{p < 0.001}^*$
Polynesia	36.957° $p = 0.085$	54.304° $\mathbf{p = 0.023}$	44.012° $\mathbf{p = 0.040}$	39.153° $p = 0.083$	47.947° $\mathbf{p = 0.024}$	–	1.867 $p = 0.078$
Utah	40.586° $p = 0.057$	59.021° $\mathbf{p = 0.016}$	30.566° $p = 0.629$	22.519° $p = 0.939$	31.962° $p = 0.620$	46.127° $\mathbf{p = 0.002}^*$	–

Lower triangle = Pairwise angle differences (in degrees) between population pairs in ontogenetic trajectories using multivariate regression, and their corresponding p-values. Upper triangle = Student's t-test results for differences between adult centroid size (log transformed). All significant differences ($p < 0.05$) are indicated in bold, and values that are significant after the sequential Bonferroni adjustment are indicated with an asterisk.

category 3 analysis, but not the adult comparison (Table 8). This result is consistent with the suggestion that the divergent temporal bone shape characteristic of adult Alaskans may not develop in this group until late adolescence. If this is the case, dietary remodeling/plasticity would be a more plausible explanation than adaptation, since the latter would likely appear during earlier stages of development. Nonetheless, this sample reveals that cold adaptation is associated with a divergent morphological pattern in adults compared with non-cold-adapted populations, likely as an adaptive and/or plastic response to a diet of tough and/or frozen foods.

Human versus nonhuman temporal bone ontogeny

The analyses conducted here help shed light on the ontogeny of the human temporal bone and provide an important contrast to analyses of African ape temporal bone ontogeny (Terhune et al., 2013) and ontogeny of the facial skeleton in humans (Strand Viðarsdóttir et al., 2002). As in these other works, ontogenetic changes in temporal bone shape are significantly correlated with size and developmental age (as indicated by the significant correlations between PC 1 and the natural log of centroid size in all populations (Table 3)). Interestingly, the general mediolateral widening of the temporal bone, deepening and anterior-posterior shortening of the glenoid fossa, and widening of the zygomatic arch revealed here among human subadults during development (Fig. 2) differs from the condition observed among African apes, but is consistent with findings in humans (Terhune et al. (2013). In contrast to humans, African apes have been described as developing a shallower glenoid fossa throughout ontogeny (Terhune et al., 2013). Terhune et al. (2013) also reported that other ape species display more laterally projecting and sagittally oriented tympanic elements throughout ontogeny, while humans experience minimal changes in tympanic shape during development. The precise explanation for these differences cannot be identified at present, but an intriguing possibility is that dietary differences between human and nonhuman apes, and their concomitant adaptive morphological changes, may play a role.

Terhune et al. (2013) further determined that subadult specimens of African apes and humans demonstrate differences in temporal bone shape early in post-natal ontogeny. Thus, hominoids achieve their adult temporal bone shape through a combination of early-appearing differences in the temporal bone and divergent ontogenetic trajectories (Terhune et al., 2013). Notably, Terhune and colleagues based their analyses on a single population of humans. Given the distinctiveness of human temporal bone morphology, this choice of a single population is unlikely to substantially influence their results, but our data do suggest that some human populations possess ontogenetic allometric trajectories that diverge significantly from those of other human populations (Table 9). In addition, some populations appear to achieve different adult temporal bone sizes; although we did not specifically assess models of heterochrony here, these differences in adult temporal bone size may have been achieved through changes in the rate and/or duration of growth.

Thus, like the results for extant hominoids from Terhune and colleagues, our data suggest that differences in adult morphology among human populations are achieved via a combination of early-arising morphological differences and divergent postnatal ontogenetic trajectories. However, the pattern of morphological differentiation among human populations is considerably less pronounced than the pattern that characterizes hominoid species. This pattern may suggest that ontogenetic trajectories generally tend to diverge more among species than among populations of a single species, although additional studies are needed in order to evaluate how labile ontogenetic trajectories are across taxonomic levels.

Temporal bone ontogeny compared with facial ontogeny

The early appearance of adult-like patterns of temporal bone correspondence among closely related populations coincides with previous results obtained for facial development (Strand Viðarsdóttir et al., 2002, Palmer and Kennedy, 1927). Similar to findings in the present study regarding the temporal bone, Strand Viðarsdóttir et al. (2002) found that subadult facial morphology reflects adult population-specific differences early in ontogeny and that variation in ontogenetic trajectories also contributes to their final adult patterns. As with temporal bone ontogenetic allometric trajectories, the population-specific ontogenetic trajectories for facial morphology also do not reflect population history (Strand Viðarsdóttir et al., 2002).

These similarities in facial and temporal bone ontogeny are interesting in light of the fact that temporal bone shape is known to reflect population history reliably in non-cold-adapted adults (Harvati and Weaver, 2006; Smith et al., 2007; Smith, 2009; von Cramon-Taubadel and Smith, 2012), while facial shape is more variable (Roseman, 2004; Harvati and Weaver, 2006; Smith, 2009). This suggests that the degree to which the morphology of a particular cranial region reflects genetic distances is independent of its ontogenetic trajectory, and that morphological differences may be established very early in ontogeny and simply magnified, regardless of whether or not the region in question is congruent with molecular variation.

Acknowledgments

HFS would like to thank Gisselle Garcia (AMNH) and Dave Hunt (NMNH) for access to Physical Anthropology collections in their care and for hospitality during data collection. We thank Una Strand Viðarsdóttir for helpful correspondence regarding her 2002 paper, Brent Adrian for comments on an earlier version of this manuscript and for assistance with figures, and Michelle Singleton for sharing her SAS code. This study was supported by start-up funds from Midwestern University to HFS.

References

Ackermann, R.R., 2002. Patterns of covariation in the hominoid craniofacial skeleton: implications for paleoanthropological models. J. Hum. Evol. 42, 167–187.
Ackermann, R.R., 2005. Variation in Neandertals: a response to Harvati (2003). J. Hum. Evol. 48, 643–646.
Adams, D.C., Collyer, M.L., 2009. A general framework for the analysis of phenotypic trajectories in evolutionary studies. Evol. 63, 1143–1154.
Adams, D.C., Otárola-Castillo, E., 2012. Package 'geomorph': Geometric Morphometric Analysis of 2d/3d Landmark Data. R Package Version 1.0.
Adams, D.C., Otárola-Castillo, E., 2013. geomorph: an R package for the collection and analysis of geometric morphometric shape data. Methods Ecol. Evol. 4, 393–399.
Allam, A.F., 1969. Pneumatization of the temporal bone. ORL J. Otorhinolaryngol. Relat. Spec. 62, 311–315.
Anderson, M.J., Ter Braak, C.J.F., 2003. Permutation tests for multi-factorial analysis of variance. J. Stat. Comput. Sim. 73, 85–113.
Babineau, T.A., Kronman, J.H., 1969. A cephalometric evaluation of the cranial base in microcephaly. Angle Orthod. 39, 57–63.
Bast, T.H., Forester, H.B., 1939. Origin and distribution of air cells in the temporal bone. Arch. Otolaryngol. 30, 183–205.
Collard, M., Wood, B.A., 2001. Homoplasy and the early hominid masticatory system: inferences from analyses of extant hominoids and papionins. J. Hum. Evol. 41, 167–194.
Collard, M., Wood, B.A., 2007. Hominin homoiology: an assessment of the impact of phenotypic plasticity on phylogenetic analyses of humans and their fossil relatives. J. Hum. Evol. 52, 573–584.
Collyer, M.L., Adams, D.C., 2007. Analysis of two-state multivariate phenotypic change in ecological studies. Ecol. 88, 683–692.
David, D.J., Hemmy, D.C., Cooter, R.D., 1990. Craniofacial Deformities: Atlas of Three Dimensional Reconstruction from Computed Tomography. Springer-Verlag, New York.
de Beer, G.R., 1937. The Development of the Vertebrate Skull. Oxford University Press, Oxford.

Eby, T.L., Nadol, J.B., 1986. Postnatal growth of the human temporal bone. Implications for cochlear implants in children. Ann. Otol. Rhinol. Laryngol. 95, 356–364.
Excoffier, L., Laval, G., Schneider, S., 2005. Arlequin ver. 3.0: an integrated software package for population genetics data analysis. Evol. Bioinformatics Online 1.
Harvati, K., Weaver, T.D., 2006. Human cranial anatomy and the differential preservation of population history and climate signatures. Anat. Rec. A 288, 1225–1233.
Howells, W.W., 1990. Micronesia to Macromongolia: micro-polynesian craniometrics and the Mongoloid population complex. Micronesia 2, 363–372.
Hylander, W.L., 1977. The adaptive significance of Eskimo craniofacial morphology. In: Dahlberg, A.A., Graber, T. (Eds.), Orofacial Growth and Development. Mouton, The Hague, pp. 129–169.
Kenna, M.A., 1996. Embryology and developmental anatomy of the ear. In: Bluestone, C.D., Stool, S.E., Kenna, M.A. (Eds.), Pediatric Otolaryngology. Saunders, Philadelphia, pp. 129–145.
Klingenberg, C.P., 2011. MorphoJ: an integrated software package for geometric morphometrics. Mol. Ecol. Resour. 11, 353–357.
Klingenberg, C.P., Montiero, L.R., 2005. Distances and directions in multidimensional shape spaces: implications for morphometric applications. Syst. Biol. 54, 678–688.
Lieberman, D.E., 1995. Testing hypotheses about recent human evolution from skulls: integrating morphology, function, development, and phylogeny. Curr. Anthropol. 36, 159–197.
Lieberman, D.E., 1997. Making behavioural and phylogenetic inferences from hominid fossils: considering the developmental influences of mechanical forces. A. Rev. Anthropol. 26, 185–210.
Lieberman, D.E., Wood, B.A., Pilbeam, D.R., 1996. Homoplasy and early *Homo*: an analysis of the evolutionary relationships of *H. habilis* sensu stricto and *H. rudolfensis*. J. Hum. Evol. 30, 97–120.
Lieberman, D.E., Ross, C.F., Ravosa, M.J., 2000a. The primate cranial base: ontogeny, function, and integration. Yearb. Phys. Anthropol. 43, 117–169.
Lieberman, D.E., Mowbray, K.M., Pearson, O.M., 2000b. Basicranial influences on overall cranial shape. J. Hum. Evol. 38, 291–315.
Lockwood, C.A., Lynch, J.M., Kimbel, W.H., 2002. Quantifying temporal bone morphology of great apes and humans: an approach using geometric morphometrics. J. Anat. 201, 447–464.
Lockwood, C.A., Kimbel, W.H., Lynch, J.M., 2004. Morphometrics and hominoid phylogeny: support for a chimpanzee-human clade and differentiation among great ape species. Proc. Natl. Acad. Sci. 101, 4356–4360.
Lycett, S.J., Collard, M., 2005. Do homoiologies impede phylogenetic analyses of the fossil hominids? An assessment based on extant papionin craniodental morphology. J. Hum. Evol. 49, 618–642.
MacPhee, R.D.E., Cartmill, M., 1986. Basicranial structures and primate systematics. In: Swindler, D.R., Erwin, J. (Eds.), Comparative Primate Biology. Liss, New York, pp. 219–275.
Mantel, N., 1967. The detection of disease clustering and a generalized regression approach. Cancer Res. 27, 209–220.
McNulty, K.P., Frost, S.R., Strait, D.S., 2006. Examining affinities of the Taung child by developmental simulation. J. Hum. Evol. 51, 274–296.
Olson, T.R., 1981. Basicrania and evolution of the Pliocene hominids. In: Stringer, C.B. (Ed.), Aspects of Human Evolution. Taylor and Francis, London, pp. 99–128.
Piras, P., Colangelo, P., Adams, D.C., Buscalioni, A., Cubo, J., Kotsakis, T., Meloro, C., Raia, P., 2010. The Gavialis-Tomistoma debate: the contribution of skull ontogenetic allometry and growth trajectories to the study of crocodylian relationships. Evol. Dev. 12, 568–579.
Relethford, J.H., 1998. Genetics of modern human origins and diversity. A. Rev. Anthropol. 27, 1–23.
Relethford, J.H., 2001. Global analysis of regional differences in craniometric diversity and population substructure. Hum. Biol. 73, 629–636.
Rice, W.R., 1989. Analyzing tables of statistical tests. Evol. 43, 223–225.
Roseman, C.C., 2004. Detecting interregionally diversifying natural selection on modern human cranial form by using matched molecular and morphometric data. Proc. Natl. Acad. Sci. 101, 12825–12829.
Rosenberg, N.A., Mahajan, S., Ramachandran, S., Zhao, C., Pritchard, J.K., Feldman, M.W., 2005. Clines, clusters, and the effect of study design on the inference of human population structure. PLoS Genet. 1, 660–671.
Scheuer, L., Black, S., 2000. Developmental Juvenile Osteology. Academic Press, San Diego.
Sherwood, R.J., 1995. The Hominin Temporal Bone: Ontogeny and Phylogenetic Implications. Ph.D. Dissertation, Kent State University.
Smith, H.F., 2009. Which cranial regions reflect genetic distances accurately in humans? Evidence from three-dimensional morphology. Am. J. Hum. Biol. 21, 36–47.
Smith, H.F., Terhune, C.E., Lockwood, C.A., 2007. Genetic, geographic, and environmental correlates of human temporal bone variation. Am. J. Phys. Anthropol. 134, 312–322.
Smith, H.F., Fisher, R.E., Everett, M.L., Thomas, A.D., Bollinger, R.B., Parker, W., 2009. Comparative anatomy and phylogenetic distribution of the mammalian cecal appendix. J. Evol. Biol. 22, 1984–1999.
Strand Viðarsdóttir, U., O'Higgins, P., Stringer, C., 2002. A geometric morphometric study of regional differences in the ontogeny of the modern human facial skeleton. J. Anat. 201, 221–229.
Terhune, C.E., Kimbel, W.H., Lockwood, C.A.L., 2013. Postnatal temporal bone ontogeny in *Pan, Gorilla, and Homo*, and the implications for temporal bone growth in *Australopithecus afarensis*. Am. J. Phys. Anthropol. 151, 630–642.
Ubelaker, D.H., 1989. The estimation of age at death from immature human bone. In: Iscan, M.Y. (Ed.), Age Markers in the Human Skeleton. Charles C. Thomas, Springfield, pp. 55–70.
von Cramon-Taubadel, N., 2009a. Revisiting the homoiology hypothesis: the impact of phenotypic plasticity on the reconstruction of human population history from craniometric data. J. Hum. Evol. 57, 179–190.
von Cramon-Taubadel, N., 2009b. Congruence of individual cranial bone morphology and neutral molecular affinity patterns in modern humans. Am. J. Phys. Anthropol. 140, 205–215.
von Cramon-Taubadel, N., 2011. The relative efficacy of functional and developmental cranial modules for reconstructing global human population history. Am. J. Phys. Anthropol. 146, 83–93.
von Cramon-Taubadel, N., Smith, H.F., 2012. The relative efficacy of cranial modules for reconstructing hominoid genetic relationships: implications for the reconstruction of hominin phylogeny. J. Hum. Evol. 62, 640–653.
Weidenreich, F., 1941. The brain and its role in the phylogenetic transformation of the human skull. Trans. Am. Phil. Soc. NS 31, 321–442.
White, T.D., Folkens, P.A., 2000. Human Osteology. Academic Press, San Diego.